Supplementary information for: Polymer-chlorosome nanocomposites consisting of non-native combinations of self-assembling bacteriochlorophylls

Gregory S. Orf[1], Aaron M. Collins[2], Dariusz M. Niedzwiedzki[3], Marcus Tank[4,5], Vera Thiel[4,5], Adam Kell[6], Donald A. Bryant[4,7], Gabriel A. Montaño[2,*], and Robert E. Blankenship[1,3,*]

[1]Departments of Chemistry and Biology, Washington University in St. Louis, St. Louis, MO 63130

[2]Center for Integrated Nanotechnologies, Los Alamos National Laboratory, Los Alamos, NM 87545

[3]Photosynthetic Antenna Research Center (PARC), Washington University in St. Louis, St. Louis, MO 63130

[4]Department of Biochemistry and Molecular Biology, The Pennsylvania State University, University Park, PA 16802, USA

[5]Department of Biological Sciences, Tokyo Metropolitan University, Tokyo, Japan 192-0397

[6]Department of Chemistry, Kansas State University, Manhattan, KS 66506, USA

[7]Department of Chemistry and Biochemistry, Montana State University, Bozeman, MT 59717

[*]To whom correspondence should be addressed: Gabriel A. Montaño (gbmon@lanl.gov) or Robert E. Blankenship (blankenship@wustl.edu)

Dynamic light scattering (DLS) for sizing of the PCNs

We measured DLS for the unary and binary PCNs to determine statistical distribution of their size. DLS revealed that each sucrose gradient-purified PCN sample had a unimodal size distribution with polydispersity indices less than 0.23. The hydrodynamic radii are generally consistent with that measured for chlorosomes[1,2], although the 1:1 *e*:*f* PCN and the 1:1 *c*:*e* PCN are smaller and larger, respectively than the clustering of the other PCNs around an average hydrodynamic radius of ~89 nm.

Table S1: DLS-derived sizing parameters for sucrose gradient-purified PCNs.

PCN Pigment Ratio	Hydrodynamic Radius (nm)	Polydispersity Index
***c* only**	80.05	0.103
***d* only**	93.15	0.091
***e* only**	80.30	0.099
***f* only**	76.05	0.184
1:1 *c*:*d*	91.00	0.230
1:1 *c*:*e*	141.2	0.210
1:1 *c*:*f*	87.50	0.097
1:1 *d*:*e*	83.95	0.210
1:1 *d*:*f*	94.15	0.214
1:1 *e*:*f*	64.75	0.115

These data, coupled with the sucrose gradient fractionation patterns shown in Fig. 2A of the main text, illustrate that the PCNs constructed here can (1) be successfully purified away from any misassembled nanocomposites during synthesis, (2) be constructed with narrow size distributions, and (3), at the mesoscale, mimic natural chlorosomes in morphology.

Circular dichroism (CD) and linear dichroism (LD) of PCN constructs

Fig. S1 shows circular dichroism spectra for each PCN and linear dichroism spectra for selected PCNs. The CD spectra (Figs. S1, A-C) each contain the distinctive sigmoidally-shaped responses that are indicative of exciton-coupled systems, including natural chlorosomes. The CD spectra, however, do not show a conservative shape; *i.e.* the positive and negative components of the sigmoid shape do not show the same intensity (see **main text**). LD spectra (overlaid with the isotropic absorption spectrum; Figs.S1, D-F) indicate long-range ordering of the BChls in each PCN, with the net Q_y dipole of BChl aggregates generally aligning along the long-axis of the PCN. This alignment is another similarity the PCN shares with natural chlorosomes.[3–5]

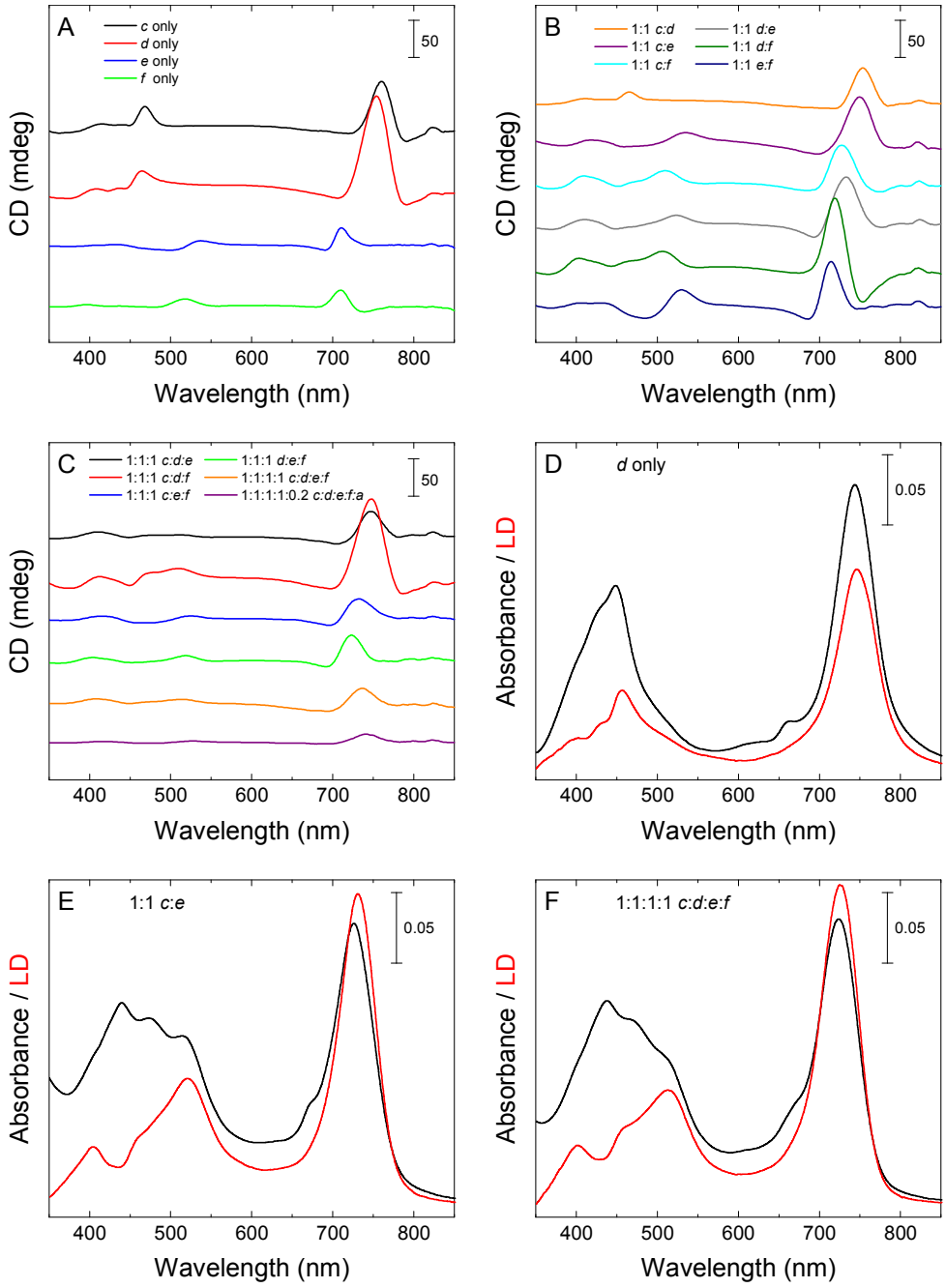

Figure S1: Circular and linear dichroism spectra of various PCN constructs. (A) CD of unary PCN's, (B) CD of binary PCN's, (C) CD of ternary, quaternary, and quinary PCN's, (D) LD/absorption spectra of a BChl *d*-only unary PCN, (E) LD/absorption spectra of a 1:1 *c*:*e* binary PCN, and (F) LD/absorption spectra of the quaternary PCN. CD spectra are offset to facilitate presentation. The LD and isotropic absorption spectra in each of (D), (E), and (F) were measured for the same sample, respectively, allowing for direct comparison.

Low temperature absorption spectroscopy of the quaternary and quinary PCN constructs

We compared the quaternary PCN to the quinary PCN via low-temperature absorption (Fig. S2). The Q_y transition in the low-temperature absorption spectrum of the quaternary PCN is narrower than at room temperature, but still smooth. In the equivalent region of the quinary PCN, the FWHM of the Q_y transition is larger than in the quaternary PCN, but still smooth. This indicates that the addition of small amounts of BChl *a* does not induce large-scale disruption of BChl *c*/*d*/*e*/*f* self-assembly, even though BChl *a* cannot self-assemble in the same mode as BChl *c*/*d*/*e*/*f* (see main text, **Discussion**).

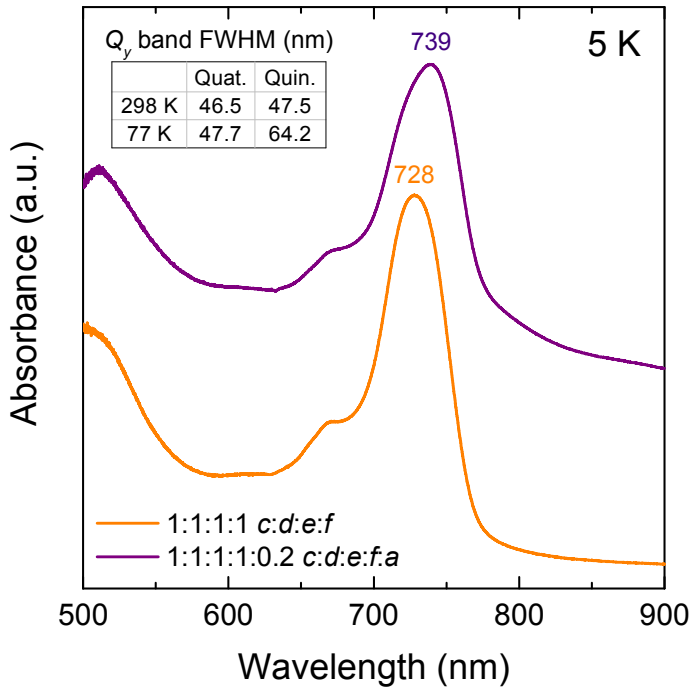

Figure S2: Absorption spectra at 5 K of the quaternary and quinary PCN samples. The quinary PCN spectrum is offset to facilitate comparison.

SI References:

(1) Tang, K.-H.; Zhu, L.; Urban, V. S.; Collins, A. M.; Biswas, P.; Blankenship, R. E. Temperature and Ionic Strength Effects on the Chlorosome Light-Harvesting Antenna Complex. *Langmuir* **2011**, *27* (8), 4816–4828.

(2) Kouyianou, K.; De Bock, P.-J.; Müller, S. A.; Nikolaki, A.; Rizos, A.; Krzyžánek, V.; Aktoudianaki, A.; Vandekerckhove, J.; Engel, A.; Gevaert, K.; Tsiotis, G. The Chlorosome of Chlorobaculum Tepidum: Size, Mass and Protein Composition Revealed by Electron Microscopy, Dynamic Light Scattering and Mass Spectrometry-Driven Proteomics. *Proteomics* **2011**, *11* (14), 2867–2880.

(3) Frese, R.; Oberheide, U.; Stokkum, I. Van; van Grondelle, R.; Foidl, M.; van Amerongen, H. The Organization of Bacteriochlorophyll c in Chlorosomes from Chloroflexus Aurantiacus and the Structural Role of Carotenoids and Protein: An Absorption, Linear Dichroism, Circular Dichroism and Stark Spectroscopy Study. *Photosynth. Res.* **1997**, *54* (2), 115–126.

(4) Garab, G.; van Amerongen, H. Linear Dichroism and Circular Dichroism in Photosynthesis Research. *Photosynth. Res.* **2009**, *101* (2–3), 135–146.

(5) Linnanto, J. M.; Korppi-Tommola, J. E. I. Investigation on Chlorosomal Antenna Geometries: Tube, Lamella and Spiral-Type Self-Aggregates. *Photosynth. Res.* **2008**, *96* (3), 227–245.